

Thermodynamics of Ion-Exchange of Alkali Metal Ions on Crystalline Niobium(V) Phosphate

Anees Ahmad,* Mohd. Rafatullah, and Md. Danish

Analytical Laboratory, Department of Chemistry, Aligarh Muslim University, Aligarh, U. P. 202 002, India

Received April 4, 2005; E-mail: aneesahmad_ana@hotmail.com

Exchange isotherms for hydrogen ion/alkali metal ions (H^+/Li^+, H^+/Na^+, H^+/K^+, H^+/Rb^+, and H^+/Cs^+) have been studied at 20, 40, and 60 °C at a constant ionic strength of 0.1 on the crystalline phase of niobium(V) phosphate. The isotherms show an irregular (S-shaped) behavior without a phase transition. A selectivity reversal has been observed over the entire system of solid compositions. Plots of the selectivity coefficient ($\log_e$ scale) versus equivalent ionic fraction of metal ion in the exchanger phase are linear for all of the systems and at all temperatures studied. The ion-exchange capacities and the maximum uptake at equilibrium is on the order of $Li^+ < Cs^+ < Rb^+ < Na^+ < K^+$. The higher selectivity of potassium ion compared to other alkali ions has been explained in terms of steric hindrance and the stiff three-dimensional structure of the exchanger having a fixed pore size. The thermodynamic parameters for the overall and for zero loading have been worked out using the Gaines–Thomas equation.

There is increasing interest in the study of synthetic inorganic ion exchangers owing to their resistance to heat and radiation. The thermodynamics of ion exchange on zirconium(IV) phosphate (abbrev: ZrP) has been studied by Baetslé and Huys, Larsen and Vissars, Amphlett, Nancollas and Tilak, Alberti, Clearfield, Boyd, Torracca, Dyer, etc.[1–20] to understand the mechanism of the ion-exchange on these materials.

The ion exchange of alkali metal ions in aqueous solutions has great significance, especially with respect to biological phenomena.[21] Therefore, special emphasis has been given to the exchange of these metal ions. Qureshi et al.[27] studied the exchange of Li^+, Na^+, and K^+ ions on niobium(V) antimonate. Abe[28] represented the thermodynamic behavior of the alkali metal ions on a crystalline phase of antimonic acid. Clearfield[29,30] has made an ion-exchange study of alkali metal ions on amorphous and crystalline phases of α-ZrP. Recently, such studies were conducted by Decaillon et al.[22] on phosphoantimonic acid and by Tanaka et al. on α-MnO_2.[23] Such studies have also been reported on tantalum(V) hydrogen phosphate[24] and niobium(V) hydroxide oxide[25] by other workers. Abe[26] published a review on the ion-exchange properties of Nb, Ta, and Sb oxides. No such study has been reported on niobium(V) phosphate.

We report in this manuscript our findings on a crystalline phase[31] of niobium(V) phosphate (abbrev: C-NbP) in the H^+-form for the exchange of alkali metal ions at 20, 40, and 60 °C. The selectivity of the hydrogen ion/alkali metal ion exchange has been studied and appropriate thermodynamic parameters have been derived. This exchanger has the molecular formula $(NbO)_2(HPO_4)_3 \cdot 6H_2O$. It is monofunctional in nature and has a theoretical ion-exchange capacity of 4.6 meq g^{-1}, which is exhibited due to the following equilibrium:

$$HPO_4^{2-} + M^+ \rightleftharpoons MPO_4^{2-} + H^+. \quad (1)$$

We have already reported[31] the IR spectra of C-NbP in the H^+-form as well as the M^+-form. A comparison of the spectra suggests that HPO_4^{2-} groups are the cation-exchange sites in this material, where the protons are exchanged with alkali metal ions (M^+). It is also evident from the said spectra that the exchanged ions are in a hydrated form. Further, the exchanger is also reported to be a strongly hydrogen-bonded three-dimensional aggregate having a fixed pore size estimated to be about 2.3 Å.

Experimental

Reagents. Diniobium pentaoxide was of B. D. H. (Poole, England). All other reagents were of analytical grade and used as received from the manufacturer.

Apparatus. The following instruments were used:

i) Rich Seifert Iso Debyeflex 2002 X-ray diffractometer for powder X-ray diffraction studies.

ii) Systronics Flame Photometer and Pye Unicam Model SP 2900 atomic absorption spectrophotometer for the analysis of alkali metal ions.

iii) Elico pH-meter for pH-measurements.

Synthesis of Crystalline Niobium(V) Phosphate. The syntheses of the exchanger, its conversion to the M^+-form and the theoretical exchange capacity have already been reported earlier.[31]

Equilibrium Studies. The isotherms for the different alkali metal ions (Li^+, Na^+, K^+, Rb^+, and Cs^+) were determined at 20, 40, and 60 °C with an accuracy of ±0.2 °C. Each point of the isotherm was determined by occasional shaking 0.1 g of C-NbP (50–100 mesh) in the H^+-form in a sealed glass tube with 10 mL of MCl + HCl solution for 8 h. Preliminary kinetic measurements showed that equilibrium was achieved much before this time. The metal-ion concentration in solution was varied from 0.0 to 10^{-1} M, while the ionic strength was kept constant (i.e., $\mu = 10^{-1}$). The alkali metals were determined by flame photometry. The Na and K ions were determined by using their respective filters, while for Cs and Rb a potassium filter was used.[32] Lithium was determined by atomic-absorption spectrometry. The concentration of each alkali metal ion at equilibrium was determined in solution as well as in the solid phases, as suggested by Bonner et al.[33]

Published on the web January 13, 2006; DOI 10.1246/bcsj.79.88

The concentration of the hydrogen ion in the solution phase was determined by pH-titration. In the solid phase, on the other hand, it was calculated from the true ion-exchange capacity (4.88 meq g^{-1}) and the concentration of the exchanged metal ion assuming a stoichiometric ion-exchange process, as suggested by Abe.[28,43,44]

X-ray diffraction patterns were taken of the different exchanged phases using Cu Kα radiation to see the effect of cation exchange on the exchanger.

All calculations of the thermodynamics parameters were made with the help of a digital computer. The least-squares method was used to find the best fit for $\ln K_H^M$ versus $\bar{X}_M$. A straight line was the best fit. The plots of Fig. 2 correspond to the fitted data, while the indicated points refer to the experimentally observed data.

Theoretical Aspects

The ion-exchange process may be represented by the following equation for hydrogen ion/univalent metal ion system:

$$\overline{RH} + M^+ \rightleftharpoons \overline{RM} + H^+, \quad (2)$$

in which R represents the C-NbP matrix and M^+ the alkali metal ion. The corrected selectivity coefficient (K_H^M) is defined by including the molar activity coefficients (γ_i) of the cations in the equilibrating solution,

$$K_H^M = \frac{\bar{X}_M \cdot X_H}{X_M \cdot \bar{X}_H} \times \frac{\gamma_H}{\gamma_M}, \quad (3)$$

where $\bar{X}_M$ and $\bar{X}_H$ refer to the equivalent ionic fraction of the alkali metal and hydrogen ions in the exchange phase, respectively. X_M and X_H refer to the corresponding equivalent fractions in the liquid phase. The ratios γ_H/γ_M are calculated from the mean ionic activity coefficients of the pure salt solutions at an ionic strength of 10^{-1} by a method of Glueckauf.[34]

The thermodynamics equilibrium constant (K) is defined by

$$K = K_H^M \cdot \frac{\overline{f_M}}{\overline{f_H}}, \quad (4)$$

where $\overline{f_M}$ and $\overline{f_H}$ are the solid-phase activity coefficients of metal and hydrogen ions, respectively, in the C-NbP. This can be evaluated by using the modified Gaines and Thomas equation,[35,36]

$$\ln K = \int_{\bar{X}_M=0}^{1} \ln K_H^M \cdot d\bar{X}_M, \quad (5)$$

assuming that the change in the activity coefficients of water in the solid and solution phases are negligible. For univalent exchange, the $\ln K_H^M$ versus $\bar{X}_M$ plots are generally linear and

$$\ln K_H^M = 4.606C\bar{X}_M + (\ln K_H^M)_{\bar{X}_M \to 0}, \quad (6)$$

where C is the Kielland coefficient. The thermodynamics equilibrium constant may be written as

$$\ln K = \ln K_H^M + 2.303C(1 - 2\bar{X}_M). \quad (7)$$

In Eq. 7, the second term on the right-hand side becomes zero for the half-exchange point (i.e., $\bar{X}_M = \bar{X}_H = 0.5$), and hence

$$\ln K = \ln K_H^M. \quad (8)$$

Thus, the numerical value of K will be equal to that of K_H^M at half exchange.

The standard free-energy change (ΔG°) for the ion-exchange equilibrium at different temperatures has been calculated by

$$\Delta G^\circ = -RT \ln K, \quad (9)$$

where R is the gas constant and T is the absolute temperature.

The ΔH° values for the different ions were calculated following Larsen[3] by the plot of $\ln K$ versus $1/T \times 10^3$ (Fig. 3). The change in entropy values was calculated by the expression

$$\Delta G^\circ = \Delta H^\circ - T\Delta S^\circ. \quad (10)$$

The enthalpy changes in inorganic ion-exchangers are generally very small,[41] and will remain constant over the temperature range studied.

Results and Discussion

The maximum uptake of ions by inorganic ion exchangers are generally less than their ion-exchange capacities, and vary extensively with the nature of the exchanging species, temperature, and concentration of the ions in solution. On the other hand, the uptake of ions in organic ion exchangers is fairly constant due to their elastic structures.[28]

The X-ray diffraction analysis of C-NbP in different cationic forms (e.g., $\overline{RLi}$, $\overline{RNa}$, $\overline{RK}$, $\overline{RRb}$, and $\overline{RCs}$) exhibits its zeolytic-type behavior where no phase transition occurs, but a slight variation of the lattice constant is observed (see Tables 1 and 2), thereby indicating a slight steric hindrance in the system.

The batch studies of ion exchange of Li^+, Na^+, K^+, Rb^+, and Cs^+ by C-NbP show the uptake of these ions as 0.70, 1.06, 1.37, 0.86, and 0.84 meq g^{-1}, respectively. Thermodynamics studies of these ions also show the same order of uptake,

Table 1. X-ray Powder Patterns of C-NbP in H^+-Form and Niobium Hydroxide Synthesized

S. No.	C-NbP			Nb-OH	
	d/Å	I/I_0	hkl	d/Å	I/I_0
1	7.23	84.6	110	7.83	
2	5.9	7.9	111	3.91	30
3	5.11	7.4	200	3.28	100
4	4.55	41	210		
5	4.15	18.4	211		
6	3.59	12	220		
7	3.23	100	310		
8	2.82	5.6	320		
9	2.72	5.6	321		
10	2.35	7.4	331		
11	2.28	43.5	420		
12	2.04	25.3	500, 430		
13	1.73	6.5	531		
14	1.61	17.9	620		
15	1.52	10.3	630, 542		
16	1.44	12.8	710, 550		
17	1.42	28.7	551, 711		
18	1.4	5.6	641, 720		
19	1.33	6.5	553, 731		
20	1.3	6.5	651, 732		
21	1.27	9.3	652, 740, 810		
22	1.13	13.6	663, 744, 841, 900		
23	1.07	13	931		
24	1.02	13	860, 1000		

Table 2. X-ray Power Patterns of C-NbP Exchanged with Alkali Metal Ions

S. No.	Li^+ ($\bar{X}_M = 0.143$)		Na^+ ($\bar{X}_M = 0.217$)		K^+ ($\bar{X}_M = 0.280$)	
	d/Å	I/I_0	d/Å	I/I_0	d/Å	I/I_0
1	7.224	85.2	7.24	89.5	7.241	88.4
2	5.92	8.5	5.98	8	5.98	7.8
3	5.1	7.4	5.12	7	5.11	7.3
4	4.55	40.1	4.55	38.5	4.55	42.1
5	4.13	18.2	4.14	17.9	4.14	18.3
6	3.6	12.2	3.6	12	3.6	12.5
7	3.22	100	3.22	100	3.22	100
8	2.81	4	2.79	5	2.83	5.2
9	2.7	4	2.72	4.9	2.75	4.9
10	2.35	7	2.35	7	2.36	7.5
11	2.28	43	2.28	43.4	2.28	43.4
12	2.04	25.5	2.03	25	2.03	25.1
13	1.73	5.9	1.74	6.8	1.74	6.5
14	1.6	17.9	1.61	17	1.62	17.5
15	1.52	9	1.55	9.5	1.53	9.8
16	1.44	11.9	1.44	12	1.44	12
17	1.42	28	1.42	28.5	1.42	27.5
18	1.4	6	1.4	6	1.4	6
19	1.32	6	1.33	6.1	1.33	6
20	1.3	6.2	1.3	6	1.3	6.8
21	1.27	9	1.27	8.9	1.27	9.2
22	1.13	13	1.14	13.5	1.14	13.5
23	1.07	13	1.07	12.8	1.07	12.5
24	1.02	12.5	1.02	13	1.02	12.5

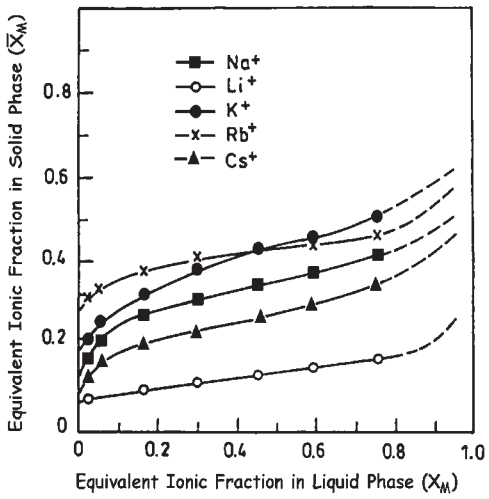

Fig. 1. Ion-exchange isotherms for H^+/alkali metal ion on C-NbP at 20 °C and ionic strength of 0.1.

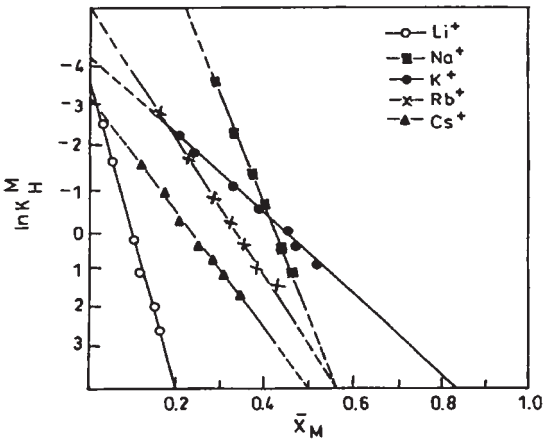

Fig. 2. Selectivity coefficients of alkali metal ion–H^+ exchange on C-NbP at 20 °C.

i.e., $Li^+ < Rb^+ < Cs^+ < Na^+ < K^+$.

Thus, C-NbP appears to have two orders of selectivity:
I. $Li^+ < Na^+ < K^+$ (parallel to ionic radii),
II. $K^+ > Rb^+ > Cs^+$ (parallel to hydrated ionic radii).
In this way, K^+ is acting as a bridge ion for the two selectivity trends, probably due to its medium ionic size and also the medium hydration number.

Ion-exchange isotherms of C-NbP for hydrogen ion/alkali metal ions exchange are given at only 20 °C (Fig. 1). They show an irregular or an S-shaped behavior without a phase transition, and hence a selectivity reversal occurs over the entire range of composition. Kielland plots (Fig. 2) are obtained by plotting $\ln K_H^M$ versus $\bar{X}_M$. They are linear at all temperatures and for all of the systems studied. The selectivity coefficients at $\bar{X}_M = 0$ and $\bar{X}_M = 1$ are calculated by extrapolation of the fitted data. The thermodynamic equilibrium constant ("K") was evaluated by the linear integration of Eq. 7 (Fig. 3).

The behavior of C-NbP for the various alkali ions is unique for each ion. A similar behavior was also reported by Clearfield et al. for zirconium(IV) phosphate.[29,30] They explained the uniqueness of the behavior based on a new thermodynamic model, which is assumed to have two types of cavities: large and small. In their model, the selectivity for the ingoing ion entirely depends upon the manner in which it

can accommodate itself inside the cavity and, of course, experiences the least steric hindrance.

The behavior of C-NbP may also be explained based on a theory developed by Barrer et al.[37,38] This theory postulates that the occupancy of an exchange site by an ion A or B affects the relative affinities of the adjacent sites for these ions.

With the progress of exchange in irregular systems, the steric hindrance for a large counter ion increases, resulting in a different, and hence energetically less favorable, occupancy of the two neighboring sites by two large ions, as compared to those of one large and one small or the two smaller ones. Based on statistical thermodynamics, Barrer gave an equation identical to that of Kielland's semiempirical relationship and defined the Kielland's empirical constant (C) by

$$C = \frac{\bar{n}_A + \bar{n}_B}{\bar{n}_Z} \times \frac{E_W}{kT}, \tag{11}$$

where the n_i's are the mole fractions of the ith species in the solid phase and E_w is the energy of interaction between the neighboring sites occupied by ions B. In this way, C is a function of interaction energy (E_w). For irregular systems, in which the occupancy of the two neighboring sites by two ions, B is *unfavorable*, the coefficient, ("C") is *negative* and also for $|C| > \ln K_H^M$ the isotherms are S-shaped and a selectivity reversal occurs. The same behavior is exhibited by C-NbP. For the H^+/Cs^+, H^+/Rb^+, and H^+/K^+ systems, $|C|$ increases in the order of $K^+ < Rb^+ < Cs^+$ and are proportional to their ionic sizes. The $|C|$ values for the H^+/Li^+, H^+/Na^+, and H^+/K^+ systems decrease with an increase of the ionic size (see Fig. 4). The lithium ion has, however, the highest $|C|$ value in spite of its lowest ionic size. On the other hand, the lowest $|C|$ value is observed for the potassium ion, though it does not possess the largest ionic size. This behavior may be attributed to the combined effect of the ionic sizes and the hydration energies of these metal ions. We can say that the pore size of the cavity and the stiffness of the matrix may be the controlling parameters causing the hindrance to the entry of the larger ions, and hence partial ion-exchange. The rubidium and cesium ions are exchanged to a lesser extent due to their larger ionic radii, while the greater hydration energies cause a lesser exchange of lithium and sodium ions. Since the potassium ion lies in between the two governing conditions in all respects, it is highly preferred by C-NbP and exchanged to a greater extent. This may be the only reason that it has the lowest $|C|$ value. The overall higher value of $|C|$ also indicates a smaller cavity in C-NbP than those of other zeolites.

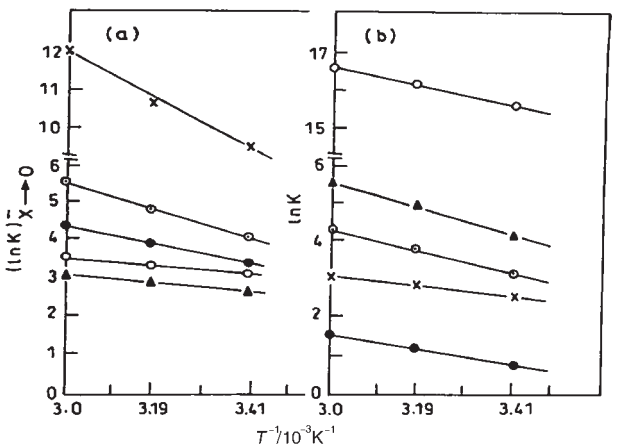

Fig. 3. Thermodynamic equilibrium constants as a function of absolute temperature. (a) For hypothetical (zero loading) i.e., $(\ln K)_{\bar{x}\to 0}$ vs $10^3/T$, (b) For overall i.e., $\ln K$ vs $10^3/T$.

In light of the above discussion, we may infer that the exchange of alkali metal ions takes place in the unhydrated form. The following may be the most probable model of exchange.

The ions reach to the surface of C-NbP where they, probably, shed most of their water of hydration at the surface of the cavity to enter into it. They again get hydrated after being exchanged at the exchange sites. With the progress of exchange, the ions become accumulated inside the cavity and cause a steric hindrance. Also, the steric hindrance is not compensated by the exchanger due to its inelastic and hence rigid matrix.

The steric hindrance is more pronounced in the case of the lithium ion, probably due to its greater hydration energy and the hydrated ionic radius compared to the rubidium and the cesium ions where the ionic sizes play the dominating role

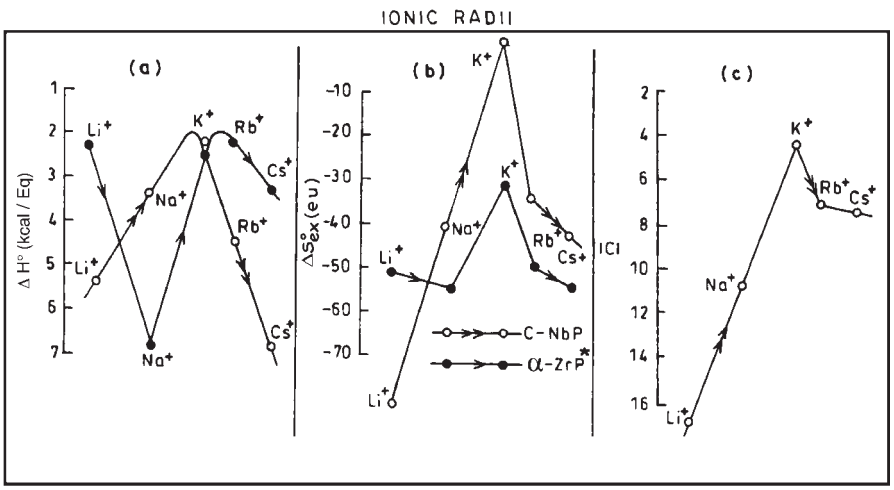

Fig. 4. Plots of ΔH°, ΔS°_{ex}, and $|C|$ (the absolute value of Kielland's coefficient) of alkali metal ions on C-NbP as a function of their ionic radii are shown in a, b, and c, respectively. ΔH° and ΔS°_{ex} on α-ZrP are shown for comparision.

Table 3.

S. No.	Equivalent ionic fraction ($\bar{X}_M$)	Selectivity sequence at 20 °C
1	0.00–0.02	$Cs^+ < Li^+ < K^+ < Rb^+ < Na^+$
2	0.02–0.17	$Li^+ < Cs^+ < K^+ < Rb^+ < Na^+$
3	0.17–0.42	$Li^+ < Cs^+ < Rb^+ < K^+ < Na^+$
4	0.42–0.57	$Li^+ < Cs^+ < Rb^+ < Na^+ < K^+$
5	0.57–0.64	$Li^+ < Cs^+ < Na^+ < Rb^+ < K^+$
6	0.64–0.93	$Li^+ < Na^+ < Cs^+ < Rb^+ < K^+$
7	0.93–1.00	$Li^+ < Na^+ < Rb^+ < Cs^+ < K^+$

Table 4. Thermodynamic Data in Tracer Concentration

Ion	Temp /°C	$(\ln K)_{X\to 0}$	ΔG° (293 K) /kcal equiv	ΔH° (293 K) /kcal equiv	ΔS° (293 K) /e.u.	$\Delta S^\circ_{hyd.}$ [a] /e.u.	ΔS°_{ex} /e.u.		
							C-NbP	α-ZrP[b]	Dowex-50[c]
Li^+	20	3.46							
	40	3.31	−2.02	−0.79	4.18	−2.4	1.78	—	—
	60	3.10							
Na^+	20	11.82							
	40	10.60	−6.88	−9.93	−10.4	5.1	−5.30	−7.9	1.9
	60	9.45							
K^+	20	4.25							
	40	3.89	−2.47	−1.89	1.99	13.6	15.59	−7.4	9.4
	60	3.29							
Rb^+	20	5.53							
	40	4.77	−3.22	−3.70	−0.91	16.5	15.58	−7.8	9.9
	60	4.02							
Cs^+	20	3.39							
	40	2.91	−1.97	−1.44	−1.13	17.2	18.33	−8.3	10.5
	60	2.83							

a) From Ref. 41. b) From Ref. 2. c) From Ref. 42.

in the lesser exchange of these ions. The hydration energy and the size of the potassium ion (hydrated ionic radius = 2.32 Å) are such that it can easily enter and best fit itself into the cavity, and can form the maximum number of ion pairs with the fixed ionogenic groups of the matrix compared to other group members. Our earlier studies on kinetics of ion exchange of alkali metal ions on C-NbP[45] also support the proposed model of ion exchange. The steric effect is also responsible for the overall partial exchange of the cations.

The selectivity sequence for the different alkali metal ions on C-NbP with the progress of exchange may be obtained from Fig. 2 and is summarized in Table 3.

Out of the above sequences of exchange, only the 4th one, which is at about half exchange, is parallel to the order of the maximum uptake, and again supports the partial exchange of alkali metal ions due to steric hindrance.

The thermodynamic parameters in a tracer concentration have also been worked out (Table 4) for these metal ions, and may be interpreted as below.

The thermodynamic equilibrium constant, at zero loadings (hypothetical) of the alkali metal ions, were obtained by backward extrapolation of the plots of Fig. 2. Thus, obtained $(\ln K_H^M)_{\bar{X}_M\to 0}$ values are then treated as described before to obtain the other thermodynamic parameters in this range (See Table 4). The order of selectivity sequence in the tracer range was found to be

$$Cs^+ < Li^+ < K^+ < Rb^+ < Na^+. \quad (12)$$

The sodium ions have a very high selectivity coefficient at "zero loading." It is on the order of 1.36×10^5 at 20 °C. Abe[28] reported a value of 2.36×10^3 on antimonic acid, while Baetslé and Huys[39] gave a value of 1.5×10^2 on zirconium(IV) phosphate.

The increasing order of entropy, enthalpy, and the negative value of the free-energy change for the alkali metals in tracer concentration range is given below:

$$\Delta S_{\bar{X}\to 0} \quad Li^+ < Cs^+ < Rb^+ < K^+ < Na^+, \quad (13)$$

$$\Delta H_{\bar{X}\to 0} \quad Li^+ < Cs^+ < Rb^+ < K^+ < Na^+, \quad (14)$$

$$\Delta G_{\bar{X}\to 0} \quad Cs^+ < Li^+ < K^+ < Rb^+ < Na^+, \quad (15)$$

$$[(\Delta S)_{ex}]_{\bar{X}\to 0} \quad Cs^+ < Li^+ < Rb^+ < K^+ < Na^+. \quad (16)$$

According to Sherry and Walton[40] the numerical values of ΔS° contribute to the entropy of hydration of the ions in aqueous solution and the entropy of exchanged cations i.e., $\Delta S^\circ_{hyd} = \Delta S^\circ_{H^+} - \Delta S^\circ_{M^+}$ and is given by:

$$M^+(aq) + H^+(gas) \rightleftharpoons M^+(gas) + H^+(aq)\Delta S^\circ_{hyd}, \quad (17)$$

and the entropy of exchange ΔS°_{ex} is given by:

$$\overline{RH^+} + M^+(gas) \rightleftharpoons \overline{RM^+} + H^+(gas). \quad (18)$$

Upon adding these two equations, we obtain the equation of

Table 5. Overall Thermodynamic Data for C-NbP

Parameters	Temp/°C	Li^+	Na^+	K^+	Rb^+	Cs^+
Ionic radius/Å		0.60	0.95	1.33	1.48	1.69
Kielland's coeff. (C)	20	−16.34	−12.27	−5.58	−7.71	−6.72
	40	−16.66	−11.69	−4.43	−7.52	−6.82
	60	−17.01	−10.82	−4.19	−7.05	−7.31
$(\ln K_H^M)_{\bar{x}_M \to 0}$	20	3.46	11.82	4.25	5.54	3.39
	40	3.31	10.62	3.89	4.47	2.91
	60	3.10	9.45	3.29	4.02	2.83
$\ln K_H^M$	20	−34.17	−16.43	−5.87	−11.68	−12.08
	40	−35.05	−16.31	−6.29	−12.54	−12.79
	60	−36.06	−15.47	−6.35	−12.21	−14.01
$\ln K$	20	−15.35	−2.30	−1.02	−3.14	−4.35
	40	−15.86	−2.85	−1.19	−3.88	−4.94
	60	−16.48	−3.01	−1.53	−4.09	−5.59
ΔG° (293 K)/kcal equiv		8.93	1.34	0.59	1.82	2.52
ΔH°/kcal equiv		−5.44	−3.45	2.47	−4.67	−6
$\Delta S_{ex}{}^\circ$/eu		−49.09	−16.36	−10.47	−22.19	−29.14
ΔS°/eu		−51.49	−11.26	3.13	−4.99	−12.64

ion exchange, i.e.

$$\overline{RH^+} + M^+ \rightleftharpoons \overline{RM^+} + H^+,$$

and

$$\Delta S^\circ = \Delta S^\circ{}_{ex} - \Delta S^\circ{}_{hyd}. \quad (19)$$

$\Delta S^\circ{}_{ex}$ thus can be calculated from this relationship of entropies. The $\Delta S^\circ{}_{hyd}$ values are obtained from Rosseinsky's table of ionic entropies of hydration.[41] The values of $\Delta S^\circ{}_{ex}$ reflect: (i) changes in the hydration of the exchanger accompanying the reaction and (ii) difference in the lattice distortion of the two forms of the exchanger. These values for this exchanger and those of α-ZrP[2] and Dowex-50[42] are listed in Table 4 for the sake of comparison. α-ZrP is a layered compound that can compensate the steric hindrance, if any, by changing its inter layer distance, and hence negative values of $\Delta S^\circ{}_{ex}$ are observed[30] for the exchange of all metal ions. On the other hand, C-NbP shows a negative $\Delta S^\circ{}_{ex}$ for Na^+ in a tracer concentration, thereby indicating the highest stability, and hence the highest selectivity, for this ion in the lower concentration range. The Na^+ ions can probably best accommodate themselves inside the cavity of the exchanger, thereby resulting least steric hindrance in the system.

The other parameters, namely, entropy, enthalpy, and free-energy, also support the higher selectivity of Na^+ in the tracer concentration range.

The overall thermodynamic parameters, on the other hand, along with the ion-exchange data, indicate the stiff three-dimensional structure for C-NbP (Table 5). It has an overall greater affinity for K^+ because of its suitable size, hydration energy, and other factors, which enable it to fit practically in the cavity of the exchanger easily and, of course, with the least steric hindrance.

The chairman department of chemistry is thanked for providing the research facility. The authors are very grateful to the reviewers for their comments in improving the manuscript.

References

1 L. H. Baetslé, D. Huys, *J. Inorg. Nucl. Chem.* **1961**, *21*, 133.
2 L. H. Baetslé, *J. Inorg. Nucl. Chem.* **1963**, *25*, 271.
3 E. M. Larsen, D. R. Vissars, *J. Phys. Chem.* **1960**, *64*, 1732.
4 C. B. Amphlett, L. A. MacDonald, *Proc. Chem. Soc.* **1962**, 276.
5 C. B. Amphlett, P. Eaton, L. A. MacDonald, A. J. Miller, *J. Inorg. Nucl. Chem.* **1964**, *26*, 297.
6 G. H. Nancollas, B. V. K. S. R. A. Tilak, *J. Inorg. Nucl. Chem.* **1969**, *31*, 3643.
7 G. Alberti, A. Conte, *J. Chromatogr.* **1961**, *5*, 244.
8 G. E. Boyd, F. Vaslow, S. Lindenbaum, *J. Phys. Chem.* **1964**, *68*, 590.
9 L. H. Baetslé, D. Huys, D. V. Deyek, *J. Inorg. Nucl. Chem.* **1966**, *28*, 2385.
10 J. P. Harkin, G. H. Nancollas, R. Paterson, *J. Inorg. Nucl. Chem.* **1964**, *26*, 305.
11 E. Torracca, *J. Inorg. Nucl. Chem.* **1963**, *31*, 1189.
12 G. Alberti, U. Costantino, M. Pelliccioni, *J. Inorg. Nucl. Chem.* **1973**, *35*, 1327.
13 L. Kulberg, A. Clearfield, *J. Phys. Chem.* **1980**, *84*, 165.
14 A. Clearfield, G. A. Day, A. Ruvarac, S. Milonjic, *J. Inorg. Nucl. Chem.* **1981**, *43*, 165.
15 P. Fletcher, R. P. Townsend, *J. Chem. Soc., Faraday Trans. 2* **1981**, *77*, 955.
16 P. Fletcher, R. P. Townsend, *J. Chem. Soc., Faraday Trans. 2* **1981**, *77*, 965.
17 A. Dyer, T. Shaheen, M. Zamin, *J. Mater. Chem.* **1977**, *7*, 1895.
18 S. A. Nabi, A. Islam, N. Rahman, *J. Adsorpt. Sci. Technol.* **1999**, *17*, 629.
19 V. I. Pet'kov, K. V. Kir'yanov, A. I. Orlova, D. B. Kitaev, *J. Therm. Anal. Calorim.* **2001**, *65*, 381.
20 D. K. Singh, N. K. Mishra, R. K. Bhardwaj, A. P. Singh, *Orient. J. Chem.* **1998**, *14*, 237.
21 J. A. Marinsky, *Ion Exchange (A Series of Advances)*,

Marcel Dekker Inc., New York, **1966**, Vol. 1, p. 228.
22 J. G. Decaillon, Y. Andres, J. C. Abbe, M. Tournoux, *Solid State Ionics* **1998**, *112*, 143.
23 Y. Tanaka, M. Tsuyi, *Solvent Extr. Ion Exch.* **1997**, *15*, 709.
24 V. A. Tarnopolskii, V. A. Ketsko, M. N. Kislitsyn, V. Yu. Kotov, A. B. Yaroslavtsev, *Zh. Neorg. Khim.* **2000**, *45*, 1625.
25 V. I. Ivanenko, I. A. Udalova, E. P. Lokshin, V. T. Kalinnikov, *Russ. J. Appl. Chem.* **2001**, *74*, 193.
26 M. Abe, T. Kotani, S. Awano, *J. Spec. Publ. R. Soc. Chem.* **1999**, *239*, 199.
27 M. Qureshi, A. P. Gupta, D. V. Nowell, J. P. Gupta, *J. Inorg. Nucl. Chem.* **1978**, *40*, 545.
28 M. Abe, *J. Inorg. Nucl. Chem.* **1979**, *41*, 85.
29 L. Kullberg, A. Clearfield, *J. Phys. Chem.* **1981**, *85*, 1578.
30 L. Kullberg, A. Clearfield, *J. Phys. Chem.* **1981**, *85*, 1585.
31 M. Qureshi, J. P. Gupta, H. Khan, A. Ahmad, *Bull. Chem. Soc. Jpn.* **1988**, *61*, 2181.
32 W. P. Thistlethwaite, *J. Inorg. Nucl. Chem.* **1966**, *28*, 2143.
33 O. D. Bonner, W. J. Argersinger, Jr., A. W. Davidson, *J. Am. Chem. Soc.* **1952**, *74*, 1044.
34 E. Glueckauf, *Nature* **1949**, *163*, 414.
35 G. L. Gaines, Jr., H. C. Thomas, *J. Chem. Phys.* **1953**, *21*, 714.
36 D. W. Breck, *Zeolites Molecular Sieves, Structure, Chemistry, and Use*, Wiley, New York, **1974**, p. 533.
37 R. M. Barrer, W. M. Meler, *Trans. Faraday Soc.* **1958**, *54*, 1074.
38 R. M. Barrer, R. Papadopoulas, L. V. C. Rees, *J. Inorg. Nucl. Chem.* **1967**, *29*, 2047.
39 L. H. Baestle, D. Huys, *J. Inorg. Nucl. Chem.* **1967**, *30*, 639.
40 H. S. Sherry, H. F. Walton, *J. Phys. Chem.* **1967**, *71*, 1457.
41 D. R. Rosseinsky, *Chem. Rev.* **1965**, *65*, 467.
42 K. A. Kraus, R. J. Raridon, *J. Phys. Chem.* **1959**, *63*, 1901.
43 M. Abe, K. Sudoh, *J. Inorg. Nucl. Chem.* **1980**, *42*, 1051.
44 M. Abe, in *Inorganic Ion Exchange Materials*, ed. by A. Clearfield, CRC Press, Boca Raton, Florida, U.S.A., **1982**, Chap. V.
45 M. Quereshi, A. Ahmad, *Solvent Extr. Ion Exch.* **1986**, *4*, 823.